

Towards High-Consistency Embodied World Model with Multi-View Trajectory Videos

Taiyi Su¹, Jian Zhu^{1*}, Yaxuan Li³, Chong Ma², Zitai Huang², Hanli Wang², Yi Xu¹

¹Midea Group

²Tongji University

³East China Normal University

Abstract

Embodied world models aim to predict and interact with the physical world through visual observations and actions. However, existing models struggle to accurately translate low-level actions (e.g., joint positions) into precise robotic movements in predicted frames, leading to inconsistencies with real-world physical interactions. To address these limitations, we propose MTV-World, an embodied world model that introduces **Multi-view Trajectory-Video** control for precise visuomotor prediction. Specifically, instead of directly using low-level actions for control, we employ trajectory videos obtained through camera intrinsic and extrinsic parameters and Cartesian-space transformations as control signals. However, projecting 3D raw actions onto 2D images inevitably causes a loss of spatial information, making a single view insufficient for accurate interaction modeling. To overcome this, we introduce a multi-view framework that compensates for spatial information loss and ensures high consistency with the physical world. MTV-World forecasts future frames based on multi-view trajectory videos as input and conditioned on an initial frame per view. Furthermore, to systematically evaluate both robotic motion precision and object interaction accuracy, we develop an auto-evaluation pipeline leveraging multimodal large models and referring video object segmentation models. To measure spatial consistency, we formulate it as an object location matching problem and adopt the Jac-card Index as the evaluation metric. Extensive experiments demonstrate that MTV-World achieves precise control execution and accurate physical interaction modeling in complex dual-arm scenarios.

1. Introduction

Recent advances in embodied intelligence have underscored the critical role of world models in enabling models to un-

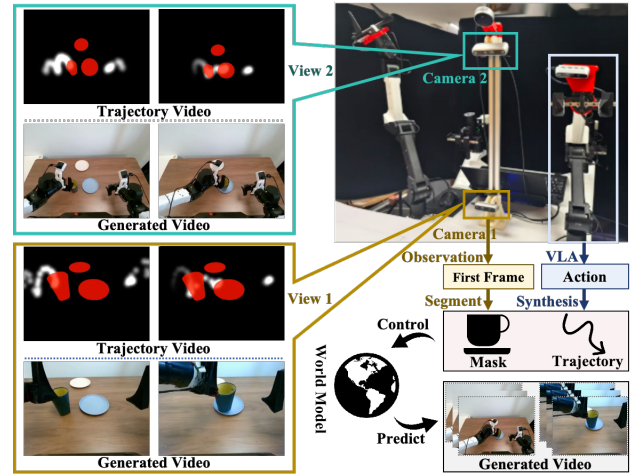


Figure 1. Overview of the proposed MTV-World, which utilizes multi-view trajectory videos as control inputs. Each trajectory video is synthesized by combining the initial object mask with trajectory motions for future frame prediction. The multi-view trajectories clearly depict the robot arm’s movement paths and its interactions with objects.

derstand, predict, and interact with their environments [5, 9, 18, 44]. An embodied world model serves as a predictive simulator of the physical world, capable of forecasting future outcomes conditioned on current observations and planned actions [1, 17, 50]. In practical applications, an embodied world model can function as a data engine [21, 22], generating diverse and controllable visual experiences to enhance policy learning, and as a policy evaluator [25, 26, 30, 49], providing a safe and efficient environment to assess and refine decision-making strategies without real-world execution.

Despite rapid progress in embodied intelligence, current embodied world models still face significant limitations. Most existing models struggle to accurately translate low-level actions (e.g., joint positions) into precise robotic motions, resulting in unstable or unrealistic arm trajectories in

*Corresponding Author (jianzhu823@gmail.com)

predicted videos. Consequently, a second challenge naturally arises: when the predicted arm motion itself is imprecise, the model cannot reliably simulate object–arm interactions, leading to inconsistencies with real-world physical dynamics.

To address these challenges, we propose MTV-World, an embodied world model that introduces Multi-view Trajectory-Video control for accurate and physically grounded visuomotor prediction, as illustrated in Figure 1. To tackle the first challenge (unrealistic arm trajectories in predicted videos), we introduce trajectory videos as explicit motion control signals. The generation of trajectory videos consists of three steps: (1) we map raw action sequences (joint positions) generated by a vision-language-action (VLA) model into Cartesian-space end-effector poses; (2) we project these end-effector poses into image-space pixel coordinates using calibrated camera intrinsic and extrinsic parameters; and (3) we render glowing points at the projected coordinates and synthesize temporally continuous trajectory videos that visualize motion evolution over time.

However, projecting 3D actions onto 2D images inevitably leads to a loss of spatial information [45], which in turn causes inconsistencies with real-world physical interactions (the second major challenge mentioned above). To alleviate this issue, we introduce two key components: (1) an object mask as a foreground prior, and (2) a multi-view framework for spatial consistency. For the first component, to explicitly model the interaction between the robotic arms and manipulated objects, we utilize an object mask from the initial frame as a foreground prior [13]. These masks are automatically obtained through a pipeline that leverages vision language model (VLM) and referring video object segmentation (RVOS) [7, 11, 27, 43]. For the second component, the multi-view framework ensures geometric consistency and captures object interactions from complementary perspectives. With these designs, MTV-World takes the multi-view trajectory videos as input and is conditioned on an initial frame per view to forecast future frames with accurate motion and consistent physical interactions.

Furthermore, to systematically evaluate both robotic motion precision and object interaction accuracy, we develop an auto-evaluation pipeline that reuses the foreground prior extraction strategy described above for perceptual judgment. To quantify spatial consistency, we formulate the evaluation as an object location matching problem and adopt the Jaccard Index between masks from the ground-truth and predicted videos as the evaluation metric [23, 33]. Additionally, since the segmentation performance of RVOS is also influenced by object semantics, it imposes higher demands on the semantic consistency of world models. Extensive experiments demonstrate that MTV-World achieves state-of-the-art performance in control accuracy and physi-

cal interaction consistency.

The major contributions of this work are summarized as follows:

- We present MTV-World, an embodied world model that introduces Multi-view Trajectory-Video control for accurate and physically consistent visuomotor forecasting.
- MTV-World utilizes trajectory videos generated from calibrated camera parameters and Cartesian-space mappings as control representations.
- A multi-view architecture is designed to mitigate spatial information loss and enhance consistency with real-world physical interactions.
- An auto-evaluation pipeline is established to assess both motion precision and object interaction accuracy via object-location matching and the Jaccard Index.

2. Related Work

2.1. World Models

Recent advances in video generation have significantly enhanced the capacity of models to simulate and understand the physical world [4, 12, 16, 36, 42, 47]. World models aim to predict future states from past observations and control actions, providing a foundation for embodied intelligence. They have been widely applied in simulated environments such as games [18, 44] and autonomous driving [14, 51]. Several recent works extend video generative models to interactive, controllable settings. Pandora [41] introduces a hybrid autoregressive–diffusion framework capable of simulating world dynamics and executing real-time text-driven control. Genie [5] learns a latent action interface from Internet videos, enabling the creation of interactive, playable environments directly from diverse visual-text prompts. RoboDreamer [48] factorizes video generation into compositional primitives conditioned on language, allowing flexible task composition for robotic manipulation. Bar *et al.* [2] focus on controllable video prediction conditioned on navigation commands, improving spatial reasoning and trajectory planning. iVideoGPT [38] generalizes this paradigm into a scalable transformer architecture that integrates visual observations, actions, and rewards into tokenized sequences for next-token prediction. RoboScape [34] incorporates physics-informed supervision via temporal depth prediction and keypoint dynamics, enhancing physical realism in video generation. The developments of world models highlight the growing potential of generative video models as general-purpose predictive simulators.

2.2. Embodied World Models

Beyond open-world video generation, embodied world models aim to predict and interact with the physical world through visual observations and actions in the context of embodied intelligence. Cosmos [1] introduces a hierarchi-

cal simulation framework that integrates instruction controllability with physical consistency. Zhu *et al.* [50] leverage both video and action signals for policy learning, capturing temporal dynamics as a powerful pretraining paradigm for multi-task data. EnerVerse-AC [22] designs a multi-level action-conditioning mechanism and ray-map encoding for dynamic multi-view image generation, improving generalization through diverse failure trajectories. FLARE [46] aligns latent features between diffusion transformers and future observations, enabling policy learning with long-horizon prediction. Wang *et al.* [37] focus on large-scale video–action modeling for generating high-quality robot learning data. Li *et al.* [24] optimize video and action prediction through a shared latent space that bridges visual and action domains, enhancing inference efficiency and accuracy. WorldVLA [6] unifies VLA modeling and world simulation within a single autoregressive framework to jointly predict actions and future visual outcomes. Ctrl-World [17] extends this direction to a controllable multi-view setting, enabling policy-in-the-loop rollouts purely within imagination space. Tesseract [45] introduces a 4D embodied video dataset with depth and surface normals for physically consistent manipulation modeling. RLVR-World [39] further combines reinforcement learning with verifiable rewards to directly optimize world models based on quantitative interaction metrics. WorldEval [26] provides an automated evaluation pipeline that encodes low-level actions into latent control representations to assess real-world robot policies online.

3. Method

3.1. Problem Formulation

The objective is to construct a world model capable of predicting and interacting with the physical world through visual observations and actions produced by a generalist robotic policy. As for a policy π (e.g., π_0 [3]), it takes multi-view visual observations and a language instruction as inputs, and outputs a sequence of control actions. At each time step t , the robot observation is represented as $o_t = [I_1^t, \dots, I_V^t, q_t]$, where $[I_1^t, \dots, I_V^t]$ denote the V camera views and q_t corresponds to the robot’s pose (e.g., joint poses). Conditioned on the current observation and an instruction l , the policy produces an action chunk of length T :

$$a_{t+1}, a_{t+2}, \dots, a_{t+T} \sim \pi(\cdot \mid o_t, l). \quad (1)$$

The world model W aims to simulate the interaction of the physical environment by predicting the perceptual outcomes resulting from executing this action sequence $A_t = [a_{t+1}, \dots, a_{t+T}]$, along with the language instruction l . Formally, W generates the corresponding future observations for each step:

$$o_{t+1}, \dots, o_{t+T} \sim W(\cdot \mid o_t, A_t, l). \quad (2)$$

3.2. Trajectory Representation

To tackle the challenge of unrealistic arm trajectories in predicted videos, we introduce trajectory videos as explicit motion control signals, as illustrated in Figure 2 (a). We first calibrate each camera to obtain its intrinsic parameters, including focal lengths f_x, f_y and principal point c_x, c_y , as well as its extrinsic parameters, represented by the camera-to-base rotation matrix R and translation vector t . We then transform the robot arm joint positions q_t into their corresponding end-effector poses in Cartesian space. Specifically, we use the forward kinematics (FK) model of a 6 degrees of freedom (6-DoF) robot defined by its Denavit–Hartenberg parameters to compute the 3D position of each point, denoted as $p_w = (x_w, y_w, z_w)$.

We project this 3D point from the robot’s base (world) coordinate system onto the 2D pixel location on the image plane. To do so, p_w is first transformed into the camera coordinate system p_c using the rotation matrix R and translation vector t obtained from camera calibration:

$$p_c = R^T(p_w - t). \quad (3)$$

The resulting camera coordinates $p_c = (x_c, y_c, z_c)$ are then projected onto the image plane through the pinhole camera model:

$$u = f_x \frac{x_c}{z_c} + c_x, \quad v = f_y \frac{y_c}{z_c} + c_y, \quad (4)$$

where f_x, f_y denote the focal lengths, (c_x, c_y) the principal point offsets encoded in the intrinsic matrix K , and (u, v) represent the projected pixel coordinates.

Finally, we synthesize trajectory videos for dual-arm motions. For each frame, the 3D end-effector positions are projected onto 2D pixel coordinates (u, v) . These projected points are drawn as fading trails of glowing points to demonstrate the continuity of motion. The frames are then composed into a single-view trajectory video X_v^{traj} , providing an intuitive visualization of the control policy. For the multi-view setting, this process is performed for each camera view, producing V synchronized trajectory videos X^{traj} .

3.3. Object Representation

To explicitly model the interaction between the robot arm and manipulated objects, we introduce an object mask from the initial frame as a foreground prior. To automatically obtain these masks, we adopt a pipeline inspired by RVOS. Specifically, we first generate textual descriptions for each object by prompting a VLM in a visual question answering (VQA) manner. Given an input image, the VLM produces a set of object descriptions, which are then provided to the RVOS model to generate segmentation masks for all objects across the entire video. The resulting full-video masks are later used for automatic evaluation, as detailed in Section 3.5.

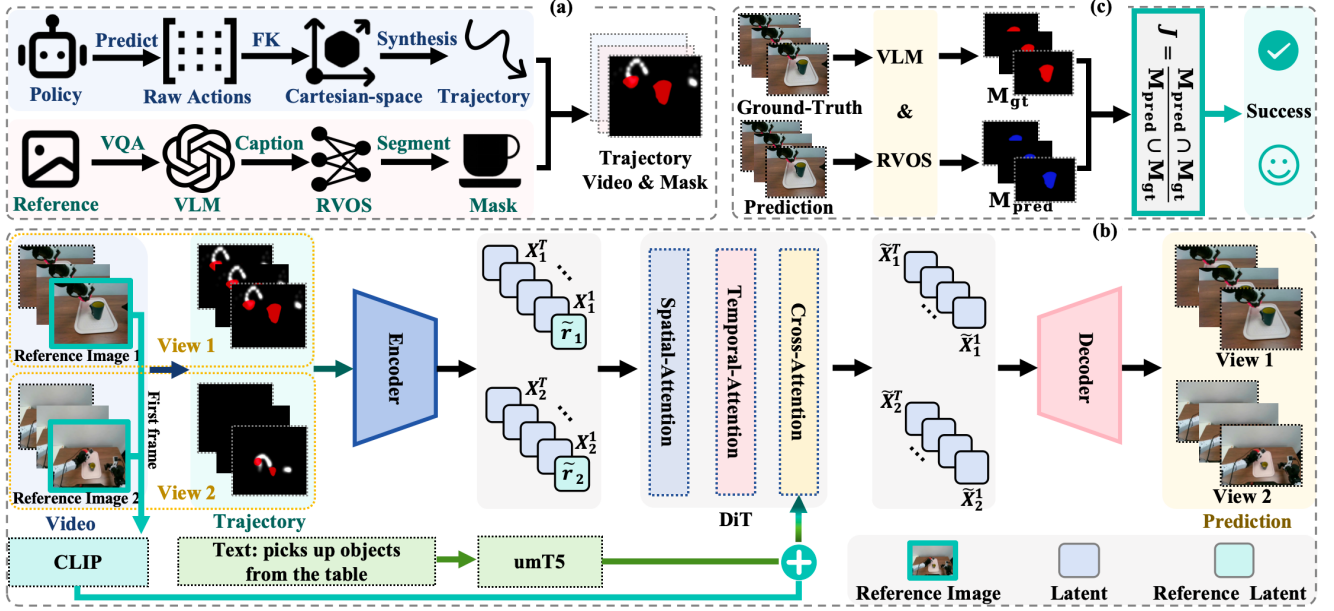


Figure 2. Illustration of the MTV-World framework. (a) Trajectory and object representation: trajectory control videos are generated by combining object masks and the trajectories of luminous points on the image to serve as control inputs. (b) MTV-World architecture: the model takes multi-view video sequences and trajectory control videos as inputs. The first frame is used as a reference image, which is simultaneously processed by CLIP for semantic encoding and by a shared VAE encoder to obtain reference latents, which are later removed before decoding. (c) Automated evaluation pipeline: performance is assessed by measuring the spatial alignment between the predicted and ground-truth object masks in videos using the Jaccard Index.

Since the world model is defined to predict future frames conditioned on the first observed frame, we utilize only the object mask extracted from the initial frame as the foreground prior. Finally, object masks in a single frame are duplicated across all frames to construct the reference mask sequence for the entire video.

3.4. Model Architecture

The overall model architecture is illustrated in Figure 2 (b). We adopt the first frame as the reference image to guide the video synthesis process. Specifically, given V synchronized camera views, the video set is denoted as $X^{\text{video}} \in \mathbb{R}^{V \times (1+T) \times 3 \times h \times w}$, where V indicates the number of views, 1 denotes the reference frame, and T denotes the number of following frames; h and w represent the frame height and width, respectively. MTV-World aims to predict future T frames for all views, conditioned on the observed initial frames and their corresponding control sequences. Both the multi-view video sequences X^{video} and the trajectory control videos X^{traj} are encoded by a shared variational autoencoder (VAE) [40] encoder into compact latent representations. Finally, the reference latent and the video latent are concatenated along the channel dimension to form the unified diffusion latent representation X used for the subsequent diffusion process.

To provide scene priors across multiple views, MTV-

World incorporates V reference images $\{I_v\}_{v=1}^V$ and a text prompt l . Each reference image is encoded by a pretrained CLIP [31] image encoder $\text{CLIP}(\cdot)$ to extract global semantic features: $F_v = \text{CLIP}(I_v)$. These features are projected into the transformer’s embedding dimension via a learned linear projection. The text prompt l is tokenized and embedded by a umT5 [10] text encoder $\text{umT5}(\cdot)$, yielding contextual tokens: $F_{\text{text}} = \text{umT5}(l)$. Finally, the projected CLIP embeddings from all views are concatenated together with the text embeddings to form a unified multimodal context: $\{F_1, \dots, F_V, F_{\text{text}}\}$. This unified multimodal context subsequently interacts with the latents through cross-attention within the diffusion transformer (DiT) [29] to ensure the incorporation of scene priors.

To ensure multi-view appearance consistency throughout the generation process, each reference image is also processed by the same VAE encoder used in the video encoding stage: $r_v = \text{Enc}(I_v)$. Here, $\text{Enc}(\cdot)$ denotes the VAE encoder. The encoded latent feature r_v is passed through a lightweight adapter $\phi(\cdot)$ to align its channel dimension with the latents as: $\tilde{r}_v = \phi(r_v)$, $\tilde{r}_v \in \mathbb{R}^{c' \times 1 \times h' \times w'}$, where c' , h' , and w' represent the channel, height, and width dimensions of the latent feature, respectively. The processed reference latents from all V views, denoted as $\{\tilde{r}_v\}_{v=1}^V$, are integrated into the latent sequence to provide cross-view appearance constraints. Specifically, for each view v , the ref-

erence latent \tilde{r}_v is concatenated with its corresponding latent sequence $X_v = [X_v^1, X_v^2, \dots, X_v^T]$ along the temporal dimension. The resulting multi-view latent set can be represented as:

$$X = \begin{bmatrix} \tilde{r}_1 & X_1^1 & X_1^2 & \dots & X_1^T \\ \vdots & \vdots & \vdots & \ddots & \vdots \\ \tilde{r}_V & X_V^1 & X_V^2 & \dots & X_V^T \end{bmatrix}, \quad (5)$$

where each row corresponds to one camera view.

After processing through all diffusion transformer layers, the output sequence $\hat{X} = \text{DiT}(X)$ preserves both the reference and generated tokens. To reconstruct the latent sequences, we remove the reference tokens and retain only the frame-wise outputs: $X_{\text{kept}} = [\hat{X}_1^1, \dots, \hat{X}_1^T; \dots; \hat{X}_V^1, \dots, \hat{X}_V^T]$. The retained tokens correspond to the predicted latent representations: $X_{\text{kept}} \in \mathbb{R}^{V \times c' \times T \times h' \times w'}$, which are decoded into the pixel space via the shared VAE decoder $\text{Dec}(\cdot)$: $X^{\text{pred}} = \text{Dec}(X_{\text{kept}})$, yielding multi-view video predictions $\{X_v^{\text{pred}}\}_{v=1}^V$ that maintain semantic alignment and visual consistency across all views.

3.5. Auto-Evaluation Pipeline

Existing evaluation methods for world models primarily rely on image- or video-based metrics such as Fréchet Inception Distance (FID) [19] and Fréchet Video Distance (FVD) [35], which mainly measure perceptual quality rather than control accuracy. However, these metrics fail to measure the accuracy of object–arm interactions or object movement.

To address these issues, we design a new automated evaluation pipeline that directly measures interactions and object movement accuracy. Specifically, we hypothesize that if a generated video accurately reproduces the robot’s manipulation and the corresponding object interactions, then the predicted object positions should closely match those in the ground-truth video.

We formulate this positional consistency as a mask-matching problem using RVOS. The segmentation masks of objects are automatically obtained for both generated and real videos. For each frame t in a video, we compute the frame-level Jaccard Index, and the overall video-level Jaccard Index is obtained by averaging across all frames:

$$\mathcal{J}_t = \frac{M_{\text{pred}}^t \cap M_{\text{gt}}^t}{M_{\text{pred}}^t \cup M_{\text{gt}}^t}, \quad \mathcal{J} = \frac{1}{T} \sum_{t=1}^T \mathcal{J}_t, \quad (6)$$

where M_{pred}^t and M_{gt}^t denote the predicted and ground-truth masks at frame t , respectively, and T is the total number of frames in the video.

The complete evaluation pipeline is fully automated, with the overall workflow depicted in Figure 2 (c). Following the procedure described in Section 3.3, we employ

Method	View 1			View 2		
	FID ↓	FVD ↓	$\mathcal{J} \uparrow$	FID ↓	FVD ↓	$\mathcal{J} \uparrow$
WorldEval [26]	–	–	–	39.0	518.2	18.3
MTV-World (w/o Mask)	25.2	43.6	51.0	19.5	69.4	39.3
MTV-World (w/ Mask)	23.2	39.1	53.9	18.2	61.1	42.0

Table 1. Comparison with baseline methods on perceptual quality (FID/FVD) and control accuracy (\mathcal{J}).

a VLM in a VQA manner to automatically generate text descriptions for each object. These descriptions are then fed into an RVOS model to produce object segmentation masks across the entire video. The resulting masks are used to compute the \mathcal{J} scores between generated and ground-truth videos, thereby enabling an end-to-end quantitative evaluation of world model performance on object-centric consistency and manipulation accuracy.

4. Experiments

4.1. Dataset and Task Setup

Dataset Overview. The experiments are conducted on a self-collected dual-arm robotic manipulation dataset containing a total of 1,492 videos across 15 real-world tasks. Each video records a complete execution sequence of two robotic arms performing coordinated manipulation behaviors. The dataset includes both successful and failed trials, with an approximate success-to-failure ratio of 8:2. In failure cases, the gripper may miss the target object but still execute the full trajectory. Introducing these failure cases further tests the model’s ability to accurately determine whether the interaction was successful.

The dataset is split into training and testing sets with a ratio of 5:5, corresponding to 748 training samples and 744 testing samples. In addition, we also evaluate training under limited-data conditions, using only 25% of the dataset (377 training samples) while keeping 50% for testing (744 samples). Results for both the standard and reduced-data settings are reported in the experiments. Additionally, we collected 395 extra videos involving only random pick-and-place tasks, which are not part of the aforementioned 15 tasks, to test the model’s zero-shot capability.

Task Setup. The dataset comprises 15 distinct manipulation tasks adapted from the RoboTwin benchmark [8, 28]: (1) Bussing Table, (2) Collect Food, (3) Collect Tableware, (4) Collect Toy, (5) Move and Stack Block AB, (6) Move and Stack Plate, (7) Move Object Two, (8) Place Block A2B Left, (9) Place Block A2B Right, (10) Place Block AB2C Left, (11) Place Block AB2C Right, (12) Place Bread Plate, (13) Place Cup Plate, (14) Shake Bottle, and (15) Stack Blocks Two.

Each task contains 97–101 videos to ensure balanced coverage. Each video includes at least two manipulable ob-

View	Model	Task ID															Overall
		1	2	3	4	5	6	7	8	9	10	11	12	13	14	15	
View 1	0% Training Data																
	MTV-World (Zero-Shot)	50.7	47.4	44.0	49.5	30.6	36.0	33.5	57.6	55.5	43.4	51.0	66.3	63.4	62.0	49.2	49.4
	25% Training Data																
	MTV-World	54.6	48.2	51.4	60.1	35.6	42.4	34.9	65.3	58.9	50.1	54.7	69.4	63.5	60.8	58.4	53.9
	50% Training Data																
	MTV-World (w/o Mask)	57.7	49.6	51.4	56.0	40.1	54.2	37.2	58.0	59.9	49.0	53.9	69.1	64.9	62.9	57.3	54.8
View 2	MTV-World (Single-View)	55.6	48.1	50.4	57.7	37.4	52.1	35.6	68.0	58.2	50.8	53.7	68.5	66.4	63.7	60.2	55.2
	MTV-World	55.7	50.7	52.4	56.1	38.7	48.9	38.6	63.5	59.8	53.1	53.8	68.3	64.2	64.5	54.6	54.9
	0% Training Data																
	MTV-World (Zero-Shot)	50.0	39.9	37.4	42.4	20.7	31.1	28.3	38.9	39.1	36.2	43.2	54.9	43.0	47.8	32.5	39.0
	25% Training Data																
	WorldEval [26]	19.9	15.3	22.8	17.6	10.8	13.8	12.0	16.6	19.9	19.7	17.2	31.5	27.3	13.2	16.7	18.3
View 2	MTV-World	52.8	43.4	40.7	51.8	23.2	34.0	26.5	45.7	41.8	40.3	45.8	56.9	42.2	43.6	42.0	42.0
	50% Training Data																
	MTV-World (w/o Mask)	56.8	43.8	40.5	48.6	26.0	41.7	30.8	40.4	42.8	39.2	43.6	57.3	43.2	43.4	41.5	42.6
	MTV-World (Single-View)	46.2	40.3	39.0	53.6	31.6	41.5	31.6	49.0	46.2	41.4	45.6	60.6	49.6	41.4	45.4	44.3
	MTV-World	54.7	47.6	44.8	50.5	27.2	39.6	32.6	46.5	46.0	43.0	45.4	58.9	48.2	50.0	40.6	45.0

Table 2. Ablation study of key components, reporting \mathcal{J} scores across individual views for 15 tasks and overall performance.

jects, excluding trays. The dataset encompasses a diverse range of object categories, such as colorful toy bricks of various sizes (blocks); plates, bowls, and cups (tableware); food items like bread, carrots, eggplants, and corn; as well as trays, which serve as collection targets or support surfaces. These tasks involve a wide range of motion primitives, including grasping, stacking, shaking, collecting, and spatial rearrangement, thereby providing a diverse benchmark for evaluating embodied manipulation models.

Robot Setup. We employ the ALOHA-style dual-arm robotic platform, named YAM, which consists of two manipulators, each with 6-DoF. This configuration results in a combined 14-dimensional state and action space for bimanual control. Two RealSense D457 cameras are mounted at different positions: one in the middle (View 1) and another at the top (View 2) to capture both close-up and global views of the manipulation scene, as illustrated in Figure 1.

Implementation Details. The proposed world model is implemented based on the Wan 2.1 framework [36]. The model is trained with an initial learning rate of 1×10^{-4} and a batch size of 4 using four NVIDIA H20 GPUs. We adopt LoRA [20] fine-tuning with a rank of 32. The training process runs for 8 epochs. Each training sample consists of two camera views, each containing 81 frames, resulting in a total of 81×2 frames per sample at a resolution of 288×384 . The text prompt is set as “The robotic arm picks up objects from the table and places them” for all tasks. We adopt Doubao v1.5 Thinking Vision [15] as the vision–language model, and SAMWISE [11] as the referring video object segmentation model.

Evaluation Criteria. We adopt FID [19] and FVD [35] to assess the perceptual quality of the generated videos. We also employ the auto-eval pipeline introduced in Section 3.5, which measures temporal and spatial consistency using the Jaccard Index \mathcal{J} [23, 33].

4.2. Baseline Comparison

We compare MTV-World with the WorldEval [26] approach, which adopts the Policy2Vec strategy for control representation. Specifically, WorldEval encodes raw action sequences into latent action vectors that guide the motion generation process. In contrast, MTV-World converts raw actions into trajectory control videos, providing a more explicit and physically grounded representation of robot behaviors.

To ensure a fair comparison, both WorldEval and MTV-World are trained on the same dataset split, using 25%/50% for training/testing, with Wan 2.1 [36] as the base model. It is important to note that WorldEval supports only single-view training and inference, whereas MTV-World is trained and evaluated under a multi-view setting. The evaluation metrics include FID, FVD, and the \mathcal{J} score.

As shown in Table 1, the proposed MTV-World significantly outperforms WorldEval across all evaluation metrics. The results demonstrate that incorporating trajectory control videos provides more stable and semantically consistent generation compared to the latent action encoding used in WorldEval. Moreover, the masked variant of MTV-World achieves the best performance, indicating that spatial masking helps the model focus on key motion regions, thereby improving both visual quality and control accuracy.

4.3. Ablation Study

We conduct comprehensive ablation experiments to systematically validate the effectiveness of the proposed MTV-World. Specifically, we investigate: (1) the impact of different trajectory representations, (2) the influence of object masking, (3) the benefits of multi-view input compared to single-view settings, (4) the zero-shot generalization ability across novel views, tasks, and objects, and (5) progress in task success rates.

Trajectory Representation. To assess the effectiveness of trajectory-based control, we compare MTV-World with the WorldEval method [26], which adopts the Policy2Vec strategy for control representation. Specifically, WorldEval encodes raw action sequences into latent action vectors to guide motion generation, while MTV-World employs trajectory-video control. As shown in Table 2, MTV-World consistently outperforms WorldEval across all tasks, demonstrating the superiority of trajectory video control over latent vector representations.

Multi-View vs. Single-View. To validate the benefits of multi-view learning, we design a Single-View variant ($V=1$), which uses only one view during both training and inference. The comparison results are presented in Table 2. In the relatively simple *View 1* scenario, the Single-View model achieves a slightly higher \mathcal{J} of 55.2, which can be attributed to its smaller input space (81 frames) compared to the 81×2 frames in the multi-view setting, leading to faster convergence on simpler scenes. However, in the more complex *View 2* scenario, its performance drops to 44.3, lagging behind the Multi-View model (45.0). Notably, the Single-View variant requires training and inference of two separate models (for View 1 and View 2), whereas MTV-World achieves multi-view consistency through a single unified model.

Zero-Shot Ability. MTV-World also exhibits strong zero-shot generalization. To evaluate this capability, we introduce an additional zero-shot dataset containing 395 samples, covering three challenging settings: (1) *View*, where entirely novel camera positions and orientations are used; (2) *Task*, where unseen manipulation tasks (e.g., random pick-and-place) are introduced; and (3) *Object*, where 50% objects do not appear in the training or testing data. As shown in Table 2, the zero-shot model achieves competitive results with 49.4 \mathcal{J} for View 1 and 39.0 \mathcal{J} for View 2. The results demonstrate remarkable generalization to unseen viewpoints, tasks, and objects.

Object Mask. We examine the effect of the *object mask* on modeling the interaction between the robot arm and the manipulated objects. As shown in Table 2, the model with the object mask consistently achieves higher \mathcal{J} scores across both views, demonstrating its effectiveness in capturing contact-aware motion dynamics. Moreover, as illus-

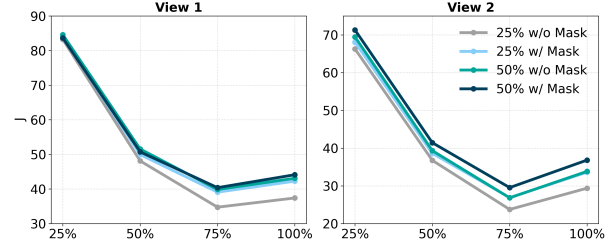


Figure 3. Success rate of object interactions over rollout progress. The x-axis denotes the rollout progress percentage, while the y-axis represents the success rate of object interactions measured by the \mathcal{J} metric.

trated in Table 1, object masking not only improves control accuracy (\mathcal{J}) but also enhances perceptual quality, as reflected by better FID and FVD metrics.

Interaction Accuracy. We further analyze how the success rate of object interactions (measured by the \mathcal{J} metric) evolves over time during rollout. As shown in Figure 3, the \mathcal{J} gradually decreases as the sequence progresses, indicating that prediction uncertainty accumulates over time. The notable drop around the 75% frame interval corresponds to the manipulation phase, where the object is often partially occluded by the robot arm, making precise prediction more challenging. Notably, the model trained with only 25% of the data achieves comparable performance to the 50%-data *w/o Mask* variant. This demonstrates that MTV-World remains robust and data-efficient even under limited supervision.

4.4. Visualization Results

Comparison with Baseline. We present qualitative comparisons with the baseline model WorldEval, as shown in Figure 4, including two representative examples of successful and failed rollouts. The first example corresponds to a successful *Stack Blocks* task, where *WorldEval* mistakenly places the block beside the target, while *MTV-World* correctly predicts the stacking action consistent with the ground truth. The second example shows a failed rollout in the *Place Bread Plate* task, where the ground-truth video demonstrates that the bread was not successfully placed onto the plate. In this case, *WorldEval* incorrectly predicts a successful placement, whereas MTV-World faithfully reproduces the failed trajectory, accurately reflecting the physical outcome.

Multi-View Trajectory Videos. We further visualize the generated multi-view trajectory videos, as illustrated in Figure 5, for two representative tasks: *Shake Bottle* (top) and *Collect Toy* (bottom). The former requires the robot to grasp and shake the cup in a circular motion. From the rendered trajectory videos, we observe that in both camera views, the glowing trajectory points form a circular trail around



Figure 4. Qualitative comparison with baseline methods, where two representative examples: a successful Stack Blocks task (top) and a failed rollout of the Place Bread Plate task (bottom) are presented.

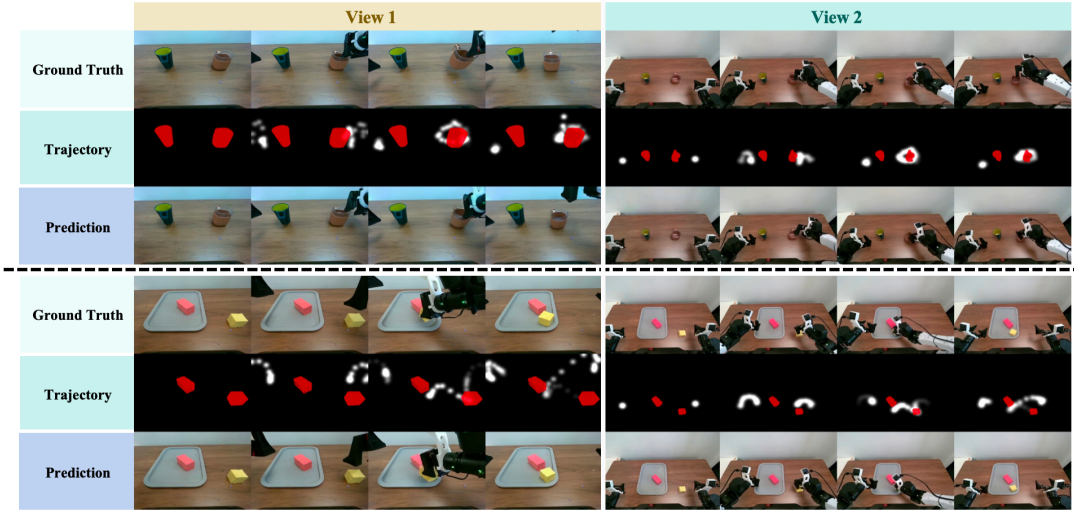


Figure 5. Visualization of the generated multi-view trajectory videos, where two examples: Shake Bottle (top) and Collect Toy (bottom), are shown.

the object’s initial mask region, indicating consistent spatio-temporal motion prediction. In the *Collect Toy* example, the temporal evolution of bright trajectory points clearly reveals the robot end-effector approaching, grasping, and placing the toy, providing an intuitive visualization of the manipulation dynamics.

5. Conclusion

In this work, we introduced MTV-World, an embodied world model that leverages Multi-view Trajectory-Video

control for precise and physically consistent visuomotor prediction. By representing control signals as trajectory videos and incorporating a multi-view framework with object-aware priors, MTV-World effectively bridges the gap between low-level actions and realistic physical interactions. Furthermore, the auto-evaluation pipeline provides a systematic and objective means to assess both motion precision and interaction accuracy. Extensive experiments demonstrate that MTV-World achieves state-of-the-art performance in complex dual-arm manipulation scenarios.

References

- [1] Niket Agarwal, Arslan Ali, Maciej Bala, Yogesh Balaji, Erik Barker, Tiffany Cai, Prithvijit Chattopadhyay, Yongxin Chen, Yin Cui, Yifan Ding, et al. Cosmos world foundation model platform for physical ai. *arXiv preprint arXiv:2501.03575*, 2025. 1, 2
- [2] Amir Bar, Gaoyue Zhou, Danny Tran, Trevor Darrell, and Yann LeCun. Navigation world models. In *Proceedings of the Computer Vision and Pattern Recognition Conference*, pages 15791–15801, 2025. 2
- [3] Kevin Black, Noah Brown, Danny Driess, Adnan Esmail, Michael Equi, Chelsea Finn, Niccolo Fusai, Lachy Groom, Karol Hausman, Brian Ichter, et al. *pi.0*: A vision-language-action flow model for general robot control. *arXiv preprint arXiv:2410.24164*, 2024. 3
- [4] Andreas Blattmann, Tim Dockhorn, Sumith Kulal, Daniel Mendelevitch, Maciej Kilian, Dominik Lorenz, Yam Levi, Zion English, Vikram Voleti, Adam Letts, et al. Stable video diffusion: Scaling latent video diffusion models to large datasets. *arXiv preprint arXiv:2311.15127*, 2023. 2
- [5] Jake Bruce, Michael D Dennis, Ashley Edwards, Jack Parker-Holder, Yuge Shi, Edward Hughes, Matthew Lai, Aditi Mavalankar, Richie Steigerwald, Chris Apps, et al. Genie: Generative interactive environments. In *Forty-first International Conference on Machine Learning*, 2024. 1, 2
- [6] Jun Cen, Chaohui Yu, Hangjie Yuan, Yuming Jiang, Siteng Huang, Jiayan Guo, Xin Li, Yibing Song, Hao Luo, Fan Wang, et al. Worldvla: Towards autoregressive action world model. *arXiv preprint arXiv:2506.21539*, 2025. 3
- [7] Ran Chen, Taiyi Su, and Hanli Wang. Wavecl: Wavelet calibration learning for referring video object segmentation. In *Proceedings of the 33rd ACM International Conference on Multimedia*, pages 3856–3864, 2025. 2
- [8] Tianxing Chen, Zhanxin Chen, Baijun Chen, Zijian Cai, Yibin Liu, Zixuan Li, Qiwei Liang, Xianliang Lin, Yiheng Ge, Zhenyu Gu, et al. Robotwin 2.0: A scalable data generator and benchmark with strong domain randomization for robust bimanual robotic manipulation. *arXiv preprint arXiv:2506.18088*, 2025. 5
- [9] Xiaowei Chi, Peidong Jia, Chun-Kai Fan, Xiaozhu Ju, Weishi Mi, Kevin Zhang, Zhiyuan Qin, Wanxin Tian, Kuangzhi Ge, Hao Li, et al. Wow: Towards a world omniscient world model through embodied interaction. *arXiv preprint arXiv:2509.22642*, 2025. 1
- [10] Hyung Won Chung, Noah Constant, Xavier Garcia, Adam Roberts, Yi Tay, Sharan Narang, and Orhan Firat. Unimax: Fairer and more effective language sampling for large-scale multilingual pretraining. *arXiv preprint arXiv:2304.09151*, 2023. 4
- [11] Claudia Cuttano, Gabriele Trivigno, Gabriele Rosi, Carlo Masone, and Giuseppe Averta. Samwise: Infusing wisdom in sam2 for text-driven video segmentation. In *Proceedings of the Computer Vision and Pattern Recognition Conference*, pages 3395–3405, 2025. 2, 6, 12
- [12] Yilun Du, Sherry Yang, Bo Dai, Hanjun Dai, Ofir Nachum, Josh Tenenbaum, Dale Schuurmans, and Pieter Abbeel. Learning universal policies via text-guided video generation. *Advances in neural information processing systems*, 36:9156–9172, 2023. 2
- [13] Yicheng Feng, Yijiang Li, Wanpeng Zhang, Sipeng Zheng, Hao Luo, Zihao Yue, and Zongqing Lu. Videorion: Tokenizing object dynamics in videos. In *Proceedings of the IEEE/CVF International Conference on Computer Vision*, pages 20401–20412, 2025. 2
- [14] Shenyan Gao, Jiazhi Yang, Li Chen, Kashyap Chitta, Yihang Qiu, Andreas Geiger, Jun Zhang, and Hongyang Li. Vista: A generalizable driving world model with high fidelity and versatile controllability. *Advances in Neural Information Processing Systems*, 37:91560–91596, 2024. 2
- [15] Dong Guo, Faming Wu, Feida Zhu, Fuxing Leng, Guang Shi, Haobin Chen, Haoqi Fan, Jian Wang, Jianyu Jiang, Jiawei Wang, et al. Seed1. 5-vl technical report. *arXiv preprint arXiv:2505.07062*, 2025. 6
- [16] Yanjiang Guo, Yucheng Hu, Jianke Zhang, Yen-Jen Wang, Xiaoyu Chen, Chaochao Lu, and Jianyu Chen. Prediction with action: Visual policy learning via joint denoising process. *Advances in Neural Information Processing Systems*, 37:112386–112410, 2024. 2
- [17] Yanjiang Guo, Lucy Xiaoyang Shi, Jianyu Chen, and Chelsea Finn. Ctrl-world: A controllable generative world model for robot manipulation. *arXiv preprint arXiv:2510.10125*, 2025. 1, 3
- [18] Danijar Hafner, Jurgis Pasukonis, Jimmy Ba, and Timothy Lillicrap. Mastering diverse control tasks through world models. *Nature*, pages 1–7, 2025. 1, 2
- [19] Martin Heusel, Hubert Ramsauer, Thomas Unterthiner, Bernhard Nessler, and Sepp Hochreiter. Gans trained by a two time-scale update rule converge to a local nash equilibrium. *Advances in neural information processing systems*, 30, 2017. 5, 6
- [20] Edward J Hu, Yelong Shen, Phillip Wallis, Zeyuan Allen-Zhu, Yuanzhi Li, Shean Wang, Lu Wang, Weizhu Chen, et al. Lora: Low-rank adaptation of large language models. *ICLR*, 1(2):3, 2022. 6
- [21] Siyuan Huang, Liliang Chen, Pengfei Zhou, Shengcong Chen, Zhengkai Jiang, Yue Hu, Yue Liao, Peng

- Gao, Hongsheng Li, Maoqing Yao, et al. Enerverse: Envisioning embodied future space for robotics manipulation. *arXiv preprint arXiv:2501.01895*, 2025. 1
- [22] Yuxin Jiang, Shengcong Chen, Siyuan Huang, Liliang Chen, Pengfei Zhou, Yue Liao, Xindong He, Chiming Liu, Hongsheng Li, Maoqing Yao, et al. Enerverse-ac: Envisioning embodied environments with action condition. *arXiv preprint arXiv:2505.09723*, 2025. 1, 3
- [23] Anna Khoreva, Anna Rohrbach, and Bernt Schiele. Video object segmentation with language referring expressions. In *Asian conference on computer vision*, pages 123–141. Springer, 2018. 2, 6
- [24] Shuang Li, Yihuai Gao, Dorsa Sadigh, and Shuran Song. Unified video action model. *arXiv preprint arXiv:2503.00200*, 2025. 3
- [25] Xuanlin Li, Kyle Hsu, Jiayuan Gu, Karl Pertsch, Oier Mees, Homer Rich Walke, Chuyuan Fu, Ishikaa Lunawat, Isabel Sieh, Sean Kirmani, et al. Evaluating real-world robot manipulation policies in simulation. *arXiv preprint arXiv:2405.05941*, 2024. 1
- [26] Yaxuan Li, Yichen Zhu, Junjie Wen, Chaomin Shen, and Yi Xu. Worldval: World model as real-world robot policies evaluator. *arXiv preprint arXiv:2505.19017*, 2025. 1, 3, 5, 6, 7
- [27] Chen Liang, Wenguan Wang, Tianfei Zhou, Jiaxu Miao, Yawei Luo, and Yi Yang. Local-global context aware transformer for language-guided video segmentation. *IEEE Transactions on Pattern Analysis and Machine Intelligence*, 45(8):10055–10069, 2023. 2
- [28] Yao Mu, Tianxing Chen, Zanxin Chen, Shijia Peng, Zhiqian Lan, Zeyu Gao, Zhixuan Liang, Qiaojun Yu, Yude Zou, Mingkun Xu, et al. Robotwin: Dual-arm robot benchmark with generative digital twins. In *Proceedings of the Computer Vision and Pattern Recognition Conference*, pages 27649–27660, 2025. 5
- [29] William Peebles and Saining Xie. Scalable diffusion models with transformers. In *Proceedings of the IEEE/CVF international conference on computer vision*, pages 4195–4205, 2023. 4
- [30] Julian Quevedo, Percy Liang, and Sherry Yang. Evaluating robot policies in a world model. *arXiv preprint arXiv:2506.00613*, 2025. 1
- [31] Alec Radford, Jong Wook Kim, Chris Hallacy, Aditya Ramesh, Gabriel Goh, Sandhini Agarwal, Girish Sastry, Amanda Askell, Pamela Mishkin, Jack Clark, et al. Learning transferable visual models from natural language supervision. In *International conference on machine learning*, pages 8748–8763, 2021. 4
- [32] Nikhila Ravi, Valentin Gabeur, Yuan-Ting Hu, Ronghang Hu, Chaitanya Ryali, Tengyu Ma, Haitham Khedr, Roman Rädle, Chloe Rolland, Laura Gustafson, et al. Sam 2: Segment anything in images and videos. *arXiv preprint arXiv:2408.00714*, 2024. 12
- [33] Seonguk Seo, Joon-Young Lee, and Bohyung Han. Urvos: Unified referring video object segmentation network with a large-scale benchmark. In *European conference on computer vision*, pages 208–223. Springer, 2020. 2, 6
- [34] Yu Shang, Xin Zhang, Yinzhou Tang, Lei Jin, Chen Gao, Wei Wu, and Yong Li. Roboscape: Physics-informed embodied world model. *arXiv preprint arXiv:2506.23135*, 2025. 2
- [35] Thomas Unterthiner, Sjoerd Van Steenkiste, Karol Kurach, Raphael Marinier, Marcin Michalski, and Sylvain Gelly. Towards accurate generative models of video: A new metric & challenges. *arXiv preprint arXiv:1812.01717*, 2018. 5, 6
- [36] Team Wan, Ang Wang, Baole Ai, Bin Wen, Chaojie Mao, Chen-Wei Xie, Di Chen, Feiwu Yu, Haiming Zhao, Jianxiao Yang, et al. Wan: Open and advanced large-scale video generative models. *arXiv preprint arXiv:2503.20314*, 2025. 2, 6
- [37] Lirui Wang, Kevin Zhao, Chaoqi Liu, and Xinlei Chen. Learning real-world action-video dynamics with heterogeneous masked autoregression. *arXiv preprint arXiv:2502.04296*, 2025. 3
- [38] Jialong Wu, Shaofeng Yin, Ningya Feng, Xu He, Dong Li, Jianye Hao, and Mingsheng Long. ivideopt: Interactive videogpts are scalable world models. *Advances in Neural Information Processing Systems*, 37: 68082–68119, 2024. 2
- [39] Jialong Wu, Shaofeng Yin, Ningya Feng, and Mingsheng Long. Rlv-world: Training world models with reinforcement learning. In *Advances in Neural Information Processing Systems*, 2025. 3
- [40] Pingyu Wu, Kai Zhu, Yu Liu, Liming Zhao, Wei Zhai, Yang Cao, and Zheng-Jun Zha. Improved video vae for latent video diffusion model. In *Proceedings of the Computer Vision and Pattern Recognition Conference*, pages 18124–18133, 2025. 4
- [41] Jiannan Xiang, Guangyi Liu, Yi Gu, Qiyue Gao, Yuting Ning, Yuheng Zha, Zeyu Feng, Tianhua Tao, Shibo Hao, Yemin Shi, et al. Pandora: Towards general world model with natural language actions and video states. *arXiv preprint arXiv:2406.09455*, 2024. 2
- [42] Zhuoyi Yang, Jiayan Teng, Wendi Zheng, Ming Ding, Shiyu Huang, Jiazheng Xu, Yuanming Yang, Wenyi Hong, Xiaohan Zhang, Guanyu Feng, et al. Cogvideox: Text-to-video diffusion models with an expert transformer. *arXiv preprint arXiv:2408.06072*, 2024. 2
- [43] Linfeng Yuan, Miaoqing Shi, Zijie Yue, and Qijun Chen. Losh: Long-short text joint prediction network

- for referring video object segmentation. In *Proceedings of the IEEE/CVF Conference on Computer Vision and Pattern Recognition*, pages 14001–14010, 2024. [2](#)
- [44] Yifan Zhang, Chunli Peng, Boyang Wang, Puyi Wang, Qingcheng Zhu, Fei Kang, Biao Jiang, Zedong Gao, Eric Li, Yang Liu, et al. Matrix-game: Interactive world foundation model. *arXiv preprint arXiv:2506.18701*, 2025. [1](#), [2](#)
- [45] Haoyu Zhen, Qiao Sun, Hongxin Zhang, Junyan Li, Siyuan Zhou, Yilun Du, and Chuang Gan. Tesseract: learning 4d embodied world models. *arXiv preprint arXiv:2504.20995*, 2025. [2](#), [3](#)
- [46] Ruijie Zheng, Jing Wang, Scott Reed, Johan Bjorck, Yu Fang, Fengyuan Hu, Joel Jang, Kaushil Kundalia, Zongyu Lin, Loic Magne, et al. Flare: Robot learning with implicit world modeling. *arXiv preprint arXiv:2505.15659*, 2025. [3](#)
- [47] Zangwei Zheng, Xiangyu Peng, Tianji Yang, Chenhui Shen, Shenggui Li, Hongxin Liu, Yukun Zhou, Tianyi Li, and Yang You. Open-sora: Democratizing efficient video production for all. *arXiv preprint arXiv:2412.20404*, 2024. [2](#)
- [48] Siyuan Zhou, Yilun Du, Jiaben Chen, Yandong Li, Dit-Yan Yeung, and Chuang Gan. Robodreamer: Learning compositional world models for robot imagination. *arXiv preprint arXiv:2404.12377*, 2024. [2](#)
- [49] Zhiyuan Zhou, Pranav Atreya, You Liang Tan, Karl Pertsch, and Sergey Levine. Autoeval: Autonomous evaluation of generalist robot manipulation policies in the real world. *arXiv preprint arXiv:2503.24278*, 2025. [1](#)
- [50] Chuning Zhu, Raymond Yu, Siyuan Feng, Benjamin Burchfiel, Paarth Shah, and Abhishek Gupta. Unified world models: Coupling video and action diffusion for pretraining on large robotic datasets. *arXiv preprint arXiv:2504.02792*, 2025. [1](#), [3](#)
- [51] Jian Zhu, Zhengyu Jia, Tian Gao, Jiaxin Deng, Shidi Li, Lang Zhang, Fu Liu, Peng Jia, and Xianpeng Lang. Other vehicle trajectories are also needed: A driving world model unifies ego-other vehicle trajectories in video latent space. *arXiv preprint arXiv:2503.09215*, 2025. [2](#)

A. Task Details

Table 5 presents the detailed descriptions, number of videos, and visualizations for all 15 manipulation tasks.

B. Consistency Analysis

Task-Level Performance Consistency. Figure 6 reports the \mathcal{J} metric across 15 tasks for multiple model variants used in the ablation study, including MTV-World (Zero-Shot), MTV-World (25% Train), MTV-World (w/o Mask), and MTV-World (Single-View). We also include the average performance curve across all five models. The results show that the performance trends across tasks remain consistent under different views.

We further sort the averaged \mathcal{J} scores for all tasks, and the rankings are shown in Tables 3 and 4. The results reveal that *Place Bread Plate* is relatively easy, achieving the highest mean score across both views. In contrast, *Move and Stack Plate*, *Move Object Two*, and *Move and Stack Block AB* consistently rank among the hardest tasks, primarily because all three require multi-step movement and placement.

Cross-View and Trajectory Consistency. We include further qualitative examples to demonstrate the consistency of the generated videos. From the visualizations in Figure 7, we observe: (1) *Cross-view consistency*: The two generated views exhibit highly consistent content. The robot arm follows identical motions across views, and the manipulated objects (the eggplant in Case 1 and the blue cube in Case 2) match precisely in position, color, and orientation. Even in situations where the prediction differs from the ground truth, the outputs across views remain perfectly aligned. (2) *Trajectory-to-video consistency*: In all examples, the robot arm motions in the generated videos closely follow the trajectories specified by the trajectory videos, demonstrating faithful execution of the control signal.

C. More Visualization

Figure 7 shows the segmentation masks used in our evaluation pipeline. The masks accurately capture object boundaries, benefiting from the strong generalization capability of the SAMWISE [11] model, which is built upon SAM 2 [32]. These accurate masks ensure reliable and consistent object-level evaluation within our auto-evaluation pipeline.

D. Limitations and Future Work

Limitations. Although MTV-World exhibits robust cross-view consistency in generating multi-view videos, it still has several limitations. First, the generation of trajectory videos relies on accurate camera intrinsics and extrinsics, which requires calibration of the cameras used in the robotic platform. While camera intrinsics can often be obtained from factory parameters, estimating extrinsics for world-coordinate transformation must still be performed manually.

Table 3. Ranking of tasks (from highest to lowest mean \mathcal{J}) under View 1.

Task ID	Task Name	\mathcal{J}
12	Place Bread Plate	68.3
13	Place Cup Plate	64.5
14	Shake Bottle	62.8
8	Place Block A2B Left	62.5
9	Place Block A2B Right	58.5
15	Stack Blocks Two	55.9
4	Collect Toy	55.9
1	Bussing Table	54.9
11	Place Block AB2C Right	53.4
3	Collect Tableware	49.9
10	Place Block AB2C Left	49.3
2	Collect Food	48.8
6	Move and Stack Plate	46.7
5	Move and Stack Block AB	36.5
7	Move Object Two	36.0

Table 4. Ranking of tasks (from highest to lowest mean \mathcal{J}) under View 2.

Task ID	Task Name	\mathcal{J}
12	Place Bread Plate	57.7
1	Bussing Table	52.1
4	Collect Toy	49.4
13	Place Cup Plate	45.2
14	Shake Bottle	45.2
11	Place Block AB2C Right	44.7
8	Place Block A2B Left	44.1
9	Place Block A2B Right	43.2
2	Collect Food	43.0
15	Stack Blocks Two	40.4
3	Collect Tableware	40.5
10	Place Block AB2C Left	40.0
6	Move and Stack Plate	37.6
7	Move Object Two	30.0
5	Move and Stack Block AB	25.7

This increases deployment difficulty and limits the applicability of our method to large amounts of readily available Internet videos that lack calibrated camera parameters. Second, while our model focuses on physical interactions between robot manipulators and objects, it currently supports only rigid-body dynamics. The predictions for deformable or soft objects remain inaccurate, highlighting a gap in modeling more complex physical behaviors.

Future Work. World models have recently become a key component in enabling closed-loop data pipelines in autonomous driving. Inspired by this direction, our future work will explore policy-in-the-loop interaction, allowing multi-step rollouts to be executed entirely within the world model’s imagination space. This integration is expected

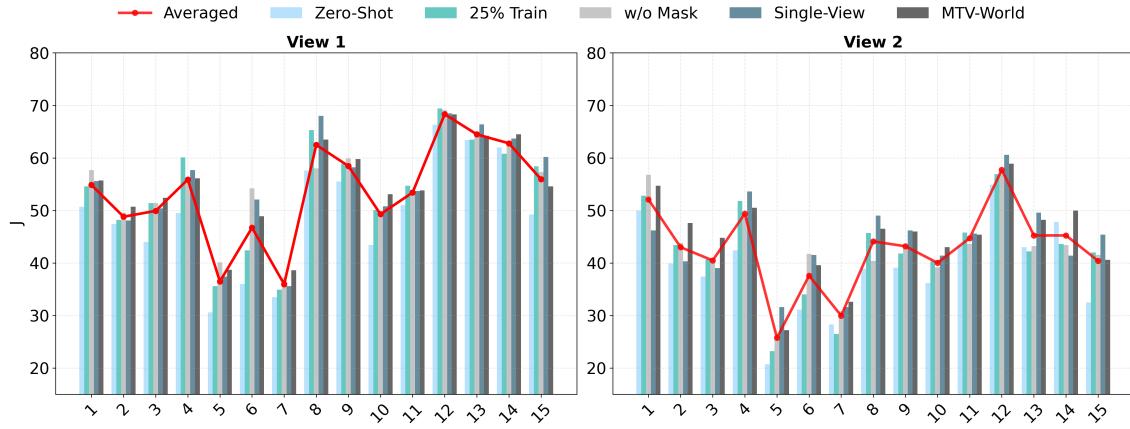


Figure 6. \mathcal{J} metric across 15 tasks for all model variants in the ablation study. The red curve denotes the averaged performance over the five variants.

to further enhance the performance of visuomotor policies, particularly for challenging corner cases that are difficult or unsafe to execute in real-world environments.

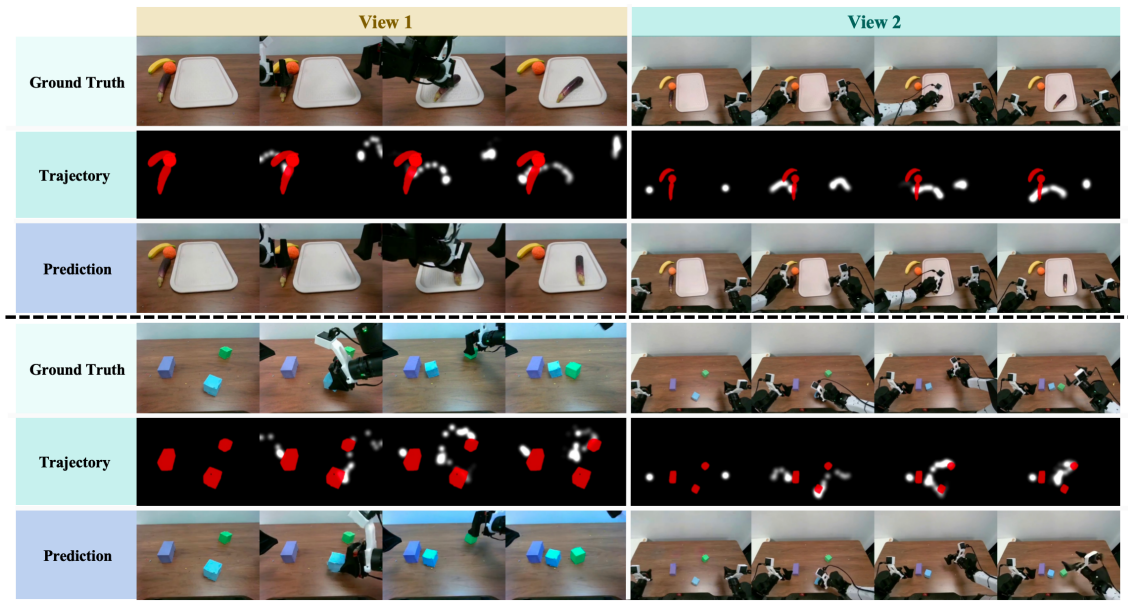







Figure 7. Visualization of the generated multi-view trajectory videos, including two cases: *Collect Food* (top) and *Place Block AB2C Right* (bottom).



Figure 8. Visualization of ground-truth videos and masks, alongside generated videos and their corresponding masks.

Table 5. Detailed descriptions and visualizations of the 15 manipulation tasks.

Task ID	Task Name	#Videos	Task Description	Frames
1	Bussing Table	97	Clear the table by placing all objects into the tray.	
2	Collect Food	97	Collect food items (bread, carrot, eggplant, etc.) and place them into the tray.	
3	Collect Tableware	101	Collect tableware (small plates, bowls, cups, etc.) into the tray.	
4	Collect Toy	100	Gather toy blocks and place them into the tray.	
5	Move and Stack Block AB	100	Move Block A to the center of the table and stack Block B on top of A.	
6	Move and Stack Plate	100	Move the small plate to the center of the table and place the block onto the plate.	
7	Move Object Two	101	Move two objects to new positions.	
8	Place Block A2B Left	100	Place Block A to the left side of Block B.	
9	Place Block A2B Right	100	Place Block A to the right side of Block B.	
10	Place Block AB2C Left	98	Place Blocks A and B to the left side of Block C.	
11	Place Block AB2C Right	100	Place Blocks A and B to the right side of Block C.	
12	Place Bread Plate	100	Place the bread onto the small plate.	
13	Place Cup Plate	100	Place the cup onto the small plate.	
14	Shake Bottle	98	Shake the bottle horizontally.	
15	Stack Blocks Two	100	Stack two blocks together.	